Biophysical Chemistry, 36 (1990) 223–234
Elsevier

BIOCHE 01452

Osmotic flow caused by polyelectrolytes

R.P.W. Williams and W.D. Comper

Biochemistry Department, Monash University, Clayton, Victoria 3168, Australia

Received 7 August 1989
Revised manuscript received 22 January 1990
Accepted 24 January 1990

Osmotic flow; Polyelectrolyte; Semipermeable membrane; Hydrodynamic frictional coefficient

Osmotic flow of water caused by high concentrations of anionic polyelectrolytes across semipermeable membranes, permeable only to solvent and simple electrolyte, has been measured in a newly designed flow cell. The flow cell features small solution and solvent compartments and an efficient stirring mechanism. We have demonstrated that, while the osmotic pressure of the anionic polyelectrolytes is determined primarily by micro-counterions, the osmotic flow is determined by solution-dependent properties as embodied in the hydrodynamic frictional coefficient which is determined by the polymer backbone segment of the polyelectrolyte. The variation of the osmotic permeability coefficient, L_p^o, with concentration and osmotic pressure closely correlated with the concentration dependence of this frictional coefficient. These studies confirm previous work that the kinetics of osmotic flow across a membrane impermeable to the osmotically active solute is primarily determined by the diffusive mobility of the solute.

1. Introduction

Osmotic flow of water is a common mechanism associated with the movement of water in biological systems such as across cell and basement membranes, and in the extracellular matrix of connective tissues, and in industrial processes, particularly those involving membrane transport. There have, in fact, been very few experimental studies on osmotic flow [1,2] and it still remains a process that is not well understood and subject to considerable discussion [3,4]. Osmotic flow is often regarded in a system where a semipermeable membrane (permeable to solvent but not to solute) separates a compartment containing a binary solution of solvent and solute and a compartment containing solvent. Water flow proceeds in the direction against the osmotic activity gradient or down the chemical potential gradient of water. The osmotic water flow is regarded as being directly proportional to the difference in osmotic pressure across the membrane. The proportionality constant has formerly been regarded in the literature as a solution-independent quantity which may be related to the geometry and structure of the membrane.

In our recent study [5] on a systematic analysis of osmotic flow generated by nonideal uncharged macromolecular solutes, we established that the proportionality constant was indeed a solution-dependent quantity related to the hydrodynamic frictional coefficient of the macromolecule. The osmotic flow could be interpreted as a series process consisting of flow across the membrane and a solute-solvent exchange process associated with the solute concentration gradient or chemical potential gradient in a thin layer immediately adjacent to the membrane. The kinetics of the flow process were demonstrated to be directly dependent on the exchange process within this layer; the slower moving solute (with higher hydrodynamical

Correspondence address: W.D. Comper, Biochemistry Department, Monash University, Clayton, Victoria 3168, Australia.

frictional coefficient) generates a lower rate of flow for a given osmotic gradient as compared to a faster moving solute.

This study sets out to investigate further the solution-dependent properties of osmotic flow with the use of polyelectrolytes. The osmotic pressure of a polyelectrolyte is not determined by the macroion but by its associated micro-counterions which have a very low hydrodynamic frictional coefficient as compared to the macroion. These polymers then offer further systematic variations to test the nature of the solution-dependent properties that may determine osmotic flow.

2. Theory

In a previous study [5], we derived the following equation for osmotic flow, J_v, across a semi-permeable membrane (permeable to water and simple electrolyte but not to macroion or polymer) that separates a compartment containing solvent (component 2) and a compartment containing a semi-dilute polymer solution (component 1) as

$$J_v = v_1(1-\phi_1)^2 \frac{M_1}{f_{12}} K\Delta\Pi \tag{1}$$

where v_1 is the partial specific volume of the polymer, ϕ_1 the volume fraction of 1, M_1 the molecular weight of 1, f_{12} the hydrodynamic frictional coefficient between polymer and solvent, and $\Delta\Pi$, the osmotic pressure of the osmotically active polymer solution. The parameter K has been assumed to be a constant. Derivation of eq. 1 was based on a series model of osmotic flow where it was suggested that the primary event driving the flow process is the diffusional exchange of solute with solvent associated with the concentration gradient of solute in a thin layer on the solution side of the membrane. The exchange process then draws water through the membrane from the solvent side. We will modify eq. 1 to account for dilute solution osmotic flows as well. In this situation, there will be two resistances controlling flow, one being associated with solute-solvent exchange, R_s, the other corresponding to hydraulic flow through the membrane, R_m. These two resistances will act in series to control total flow so that

$$J_v = (1/(R_s + R_m))\Delta\Pi \tag{2}$$

With zero hydrostatic pressure gradients across the membrane we have also defined osmotic flow in terms of the hydraulic permeability coefficient L_p^o such that

$$J_v = L_p^o \Delta\Pi \tag{3}$$

where L_p^o is equal to the reciprocal of the sum of the two resistances. In the case of macromolecular solutes in semi-dilute solutions it had been assumed that the resistance provided by the exchange process, R_s, will be the major component of this total resistance. In the case of an hydraulic flow experiment with $\Delta\Pi = 0$, an hydraulic permeability coefficient, L_p, is obtained which represents the filtration of solvent through the membrane, equal to $1/R_m$ with

$$J_v = L_p \Delta\Pi \tag{4}$$

It has previously often been assumed that $L_p^o = L_p$, however, the approach taken here suggests that L_p^o should be lower than L_p due to the influence of the solution-dependent resistances embodied in R_s (eq. 2). We further define K in eq. 1, which describes the geometric properties of the solute-solvent exchange, as

$$K = A/l \tag{5}$$

where A is the effective area of the membrane and l represents the distance over which the osmotic solute-solvent exchange process takes place. Given these relationships R_s may be described as

$$R_s = 1/\left(v_1(1-\phi_1)^2 K M_1/f_{12}\right) \tag{6}$$

Therefore, with eqs 5, 2 and 3, the relationship between L_p^o and f_{12} becomes

$$L_p^o = 1/\left[1/L_p + 1/\left(v_1(1-\phi_1)^2 K M_1/f_{12}\right)\right] \tag{7}$$

The use of eqs 3 and 7 for osmotic flow generated by a polyelectrolyte is based on treating the component as an electroneutral species and component 2 as a mixed solvent of water and simple electrolyte. This is not a serious assumption as

electrolyte dissipation associated with the polyelectrolytes used in this study is small [6,7]. These equations delineate the thermodynamic and hydrodynamic parameters of the polyelectrolyte contributing to osmotic volume flow. The hydrodynamic quantity can be estimated independently, by sedimentation experiments, and used in the osmotic flow analysis as has been done previously [5] (see also the appendix).

3. Experimental

3.1. Materials

3.1.1. Chemicals

The polymers dextran T70 and T500 together with dextran sulfate T500 ($M_w \sim 500\,000$) were supplied by AB Pharmacia (Uppsala, Sweden). Chondroitin sulfate proteoglycan subunit was prepared from Swarm rat chondrosarcoma tumors as described previously [8]. The physicochemical properties of these polymers have been described elsewhere [8,9].

3.1.2. Membranes

Nuclepore UF type C polyester membranes, MWCO ~ 1000 (lot no. 286-120) were from Nuclepore Corp., Pleasanton, CA. The L_p value for the membrane was 10.97×10^{-11} cm^3 dyn^{-1} s^{-1}.

3.2. Methods

3.2.1. Preparation of solutions

All polymer solutions were dialyzed extensively against phosphate-buffered saline which consisted of 0.14 mol dm^{-3} of NaCl, 2.68×10^{-3} mol dm^{-3} of KCl, 1.5×10^{-3} mol dm^{-3} of KH_2PO_4 and 8.1×10^{-3} mol dm^{-3} of Na_2HPO_4, pH 7.5, before use. The concentration of the polyelectrolytes in thermodynamic equilibrium with the phosphate-buffered saline was determined by solution density measurements on a DMA 55 density meter (Anton Paar, Graz, Austria) corrected for salt exclusion as predicted by the modified Manning theory [10]. The partial specific volume of proteoglycan in this buffer was estimated to be 0.490 ml g^{-1} (estimated from 5 measurements over the concentration range 18–45 kg m^{-3}) and for dextran sulfate in 0.15 mol dm^{-3} NaCl it was 0.454 ml g^{-1} (estimated from 5 measurements over the concentration range of 26–84 kg m^{-3}). The accuracy of the density meter with respect to these polyelectrolyte solutions is to the level of 0.03–0.04 kg m^{-3}. The correction for salt exclusion by the modified Manning theory resulted in a small change (5–7%) in polymer concentration.

In addition, dextran and dextran sulfate concentration was determined by optical rotation whereas chondroitin sulfate proteoglycan concentration was determined by uronic acid content by an automated carbazole method [11] using a conversion factor of dry weight/uronic acid mass of 3.29 [8].

3.2.2. Osmotic pressure of solutions

3.2.2.1. Sedimentation – equilibrium

The sedimentation-equilibrium method was used to measure the osmotic activity of the proteoglycan at low concentrations. The osmotic pressure (Π) can be described by the virial expansion

$$\Pi = RT\left[\frac{C_1}{M_1} + A_2C_1^2 + A_3C_1^3 + \ldots\right] \tag{8}$$

where R is the gas constant, T the absolute temperature, C_1 the concentration of proteoglycan in g ml^{-1}, M_1 the molecular weight and A_2 and A_3 the standard second and third virial coefficients, respectively. In the sedimentation-equilibrium experiment we have [12]

$$\frac{\omega^2 C_1(1-v_1\rho)}{2RT(\mathrm{d}C_1/\mathrm{d}r^2)} = \frac{\mathrm{d}\Pi}{\mathrm{d}C_1} = \frac{1}{M_1} + 2A_2C_1 + 3A_3C_1^2 + 4A_4C_1^3 + \ldots \tag{9}$$

where ω is the angular velocity, r the radius of rotation, v_1 the partial specific volume of the proteoglycan and ρ the solution density. The technique employed was essentially that described by Nichol et al. [13] where the solute concentration at the meniscus is very low. Analysis of the photographs at equilibrium was performed by using a digitizer (GTCO Corp., Rockville) and then fitting

the dC_1/dr data of the entire schlieren trace into eq. 9 by a polynomial regression. This was performed using a univariate curvilinear regression model with orthogonal polynomials on a Vax model 11/780 computer (Digital Equipment Corp., U.S.A.). The virial coefficients so obtained (taken to the fifth order) were used in eq. 8 to evaluate the variation of Π with C_1.

3.2.2.2. Sedimentation – diffusion

The osmotic pressure of the polyelectrolyte solutions at high concentration can be obtained from the sedimentation-diffusion data using the equation [9]:

$$\left(\frac{\partial \Pi}{\partial C_1}\right)_{T,\mu_2} = \frac{D_1(1-\rho v_1)}{S_1(1-\phi_1)} \qquad (10)$$

where D_1 and S_1 denote the mutual diffusion coefficient and the sedimentation coefficient of 1, respectively. The $\partial\Pi/\partial C_1$ data was then fitted to a polynomial regression as described earlier and the virial coefficients so obtained were used in eq. 8 to evaluate Π. For the proteoglycan subunit (PGS) the sedimentation-diffusion data was from Comper and Williams [8] and for dextran sulfate the sedimentation-diffusion data are included in table 1.

Table 1

Sedimentation data of dextran sulfate in thermodynamic equilibrium with 0.15 mol dm^{-3} NaCl

C_1 (kg m^{-3})	S_1 ($\times 10^{-13}$) (s)
25.1	2.41
42.1	1.50
48.1	1.36
53.2	1.32
69.8	1.02
84.5	0.87

Mutual diffusion coefficient data of dextran sulfate in thermodynamic equilibrium with 0.15 mol dm^{-1} NaCl

C_1 (kg m^{-3})	D_1 (10^{-11}) (m^{-2} s^{-1})
23.7	6.92
40.5	12.03
51.1	13.04
66.7	15.27
81.1	17.48

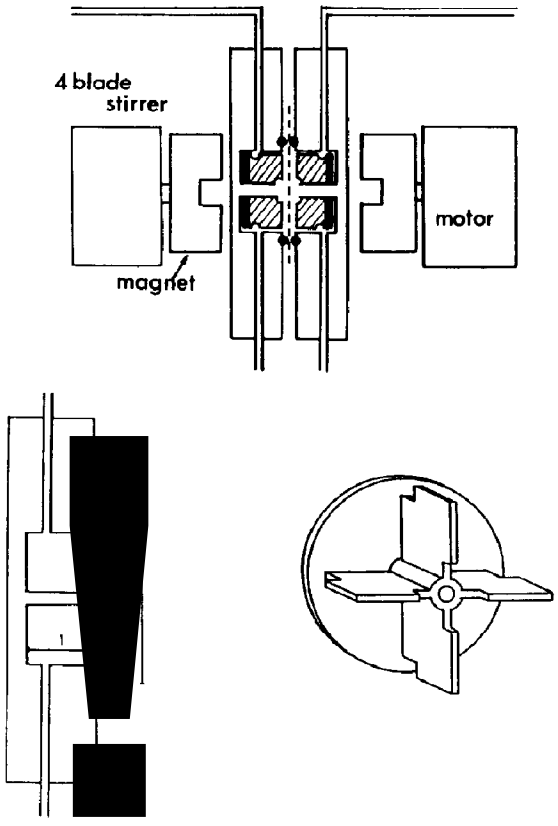

Fig. 1. Schematic diagram of osmotic cell. Distance between membrane and stirrer was less than 0.5 mm. (Bottom left) Side-on view of single compartment showing dimensions: (1) depth of compartment (10 mm), (2) width of axle (3 mm), (3) diameter of compartment (20 mm), (4) inner diameter of O ring (22 mm), (5) outer diameter of O ring (25 mm). (Bottom right) Stirrer device showing the four blades and magnetic base, 19.5 mm diameter × 9.5 mm deep.

3.2.3. Osmotic flow measurements

Osmotic flows were measured in a bivalve perspex cell that incorporated a membrane, of exposed surface area of 3.14 cm^2, to separate a compartment that contained solvent and another that contained the osmotically active solute solution (fig. 1). The cell is similar to one used previously [5] but modified to ensure more efficient stirring, to allow for the measurement of molecular fluxes and to operate at reduced solution volumes. The cell consisted of two identical cylindrical chambers, 20 mm in diameter and 10 mm

deep. Each side was fitted with a neoprene 'O' ring of 23.5 mm diameter and the two were fixed to each other by four brass bolts through flanges outside the chambers. Both sides of the cell were fitted with a four-blade 'paddle wheel' stirrer, 19.5 mm in diameter and 9.5 mm in length (total volume 1.125 cm^3), mounted on a central spindle. The stirrers were within 0.5 mm of the membrane surface. The stirrers, containing perspex covered magnets, were rotated from outside the cell by a magnet mounted on electric motors. Stirrer speed, as determined by a stroboscope, was 200 rpm. The speed was not significantly affected by the most concentrated polymer solutions used. Each half of the cell was fitted with an inlet and outlet sampling port allowing the simultaneous filling or emptying of the two sides of the cell. Prior to assembling the cell all solutions and solvent were deaerated and the membrane deaerated in solvent. The enhanced stirring efficiency achieved in this cell arises from the size of the stirrer relative to the solution chamber, and its proximity to the membrane. The design of this stirring system results in a more efficient system as compared to cells used for similar experiments by Schultz et al. [2] where the stirrer was 1.55 mm from the membrane. The membrane was always used in the vertical position and all experiments were performed in a temperature-controlled room at 20 ± 0.2 °C.

A number of experimental protocols were employed. Kinetic analysis of the osmotic flow across the membrane was performed by continuously recirculating the solution through the cell compartment, a stirred reservoir to maintain zero hydrostatic head across the membrane, and the density meter. In another arrangement, capillary bore glass tubing of 1.75 mm internal diameter was connected to each compartment to equalise hydrostatic pressure. The time-dependent change in volume in each compartment could be accurately monitored by the movement of the meniscus in each tube. The forward and reverse volume flows in different tubes were identical. The volume flow is shown to be essentially linear over a 60 min period and is in good agreement with the kinetic results from density analysis (fig. 2). The reduction in dextran concentration was only 4.0% over this period. The fact that the data extrapolate to the origin demonstrates that there is essentially zero net flow associated with the stirring mechanism. For more routine analysis, the solutions were removed from the cell after 1 h and their densities determined, volume flow being registered in the capillary tube. For the density measurements the quantity of water transferred across the membrane was calculated from the initial and final densities of the osmotically active solution. In general, changes in solute concentration in the solution compartment varied between 5 and 12% over the 1 h period.

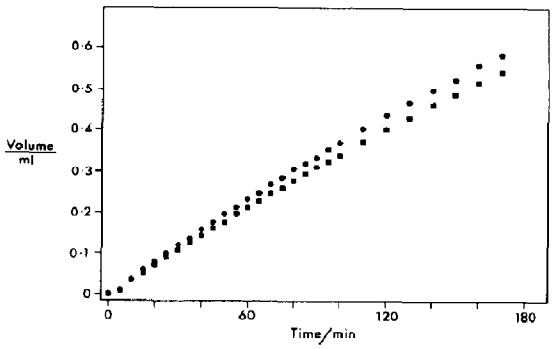

Fig. 2. Kinetics of osmotic volume flow as determined by continuous density measurements (■) and by capillary volume flow (●) (see section 3.2.3) for an experiment with a stirred solution of dextran T70 at an initial concentration of 110.4 kg m^{-3} on the solution side of a Nuclepore MWCO 1000 membrane.

In all the experiments reported here we used a Nuclepore MWCO 1000 membrane. The smooth surface of the membrane always faced the solution side.

3.2.4. Hydrodynamic frictional coefficient

The hydrodynamic frictional coefficients were determined by sedimentation velocity experiments at speeds ranging from 44000 to 56000 rpm at 20 °C in the analytical ultracentrifuge. The sedimentation coefficient (S_1) was measured by monitoring the movement of material sedimenting away from the meniscus. Normally, the solutions are so concentrated that the concentration gradient that develops refracts the light completely out of the cell. The result is that a band develops that moves according to the sedimentation of the material.

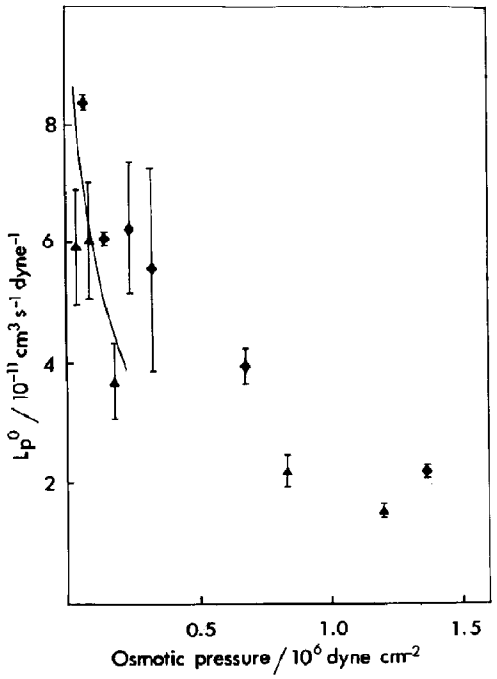

Fig. 3. Variation of the osmotic permeability coefficient, L_p^o calculated from eq. 3 of a Nuclepore MWCO 1000 membrane as a function of the osmotic pressure of dextran T70 for the stirred (◆) and unstirred system (▲) as compared to previous data (———) [5]. Data is shown as means with standard deviations ($n = 3$).

The sedimentation rate was recorded by monitoring the movement of the band median by a series of 10 photographs taken over time period of up to 48 h. Measurements of the movement of the front or back of the band yielded sedimentation coefficients very similar to those of the movement of the median. The accuracy of the sedimentation coefficient measurement was within $\pm 3\%$. S_1 is directly related to f_{12} through the following equation [8,9]:

$$S_1 = (1 - \rho v_1)(1 - \phi_1) M_1 / f_{12} \qquad (11)$$

3.2.5. Diffusion coefficients

Mutual diffusion coefficients were measured by free diffusion in a Beckman model E analytical ultracentrifuge using the schlieren optical system as described previously [8,9].

4. Results

4.1. Osmotic permeability coefficient, L_p^o, measured in newly designed osmotic flow cell

A new osmotic flow cell was designed primarily to enhance stirring efficiency and reduce sample volume as compared to a previous model. The values obtained for the osmotic permeability coefficient of dextran T70 as a function of osmotic pressure are shown in fig. 3. The results are given as means of multiple experiments with the standard deviations of the means shown as error bars. There is a marked decrease in L_p^o with increasing osmotic pressure which is in agreement with our previous studies [5] together with the fact that there appears to be a small separation between the results of the stirred and unstirred systems. The lack of any significant anomalous behaviour associated with unstirred layers is further substanti-

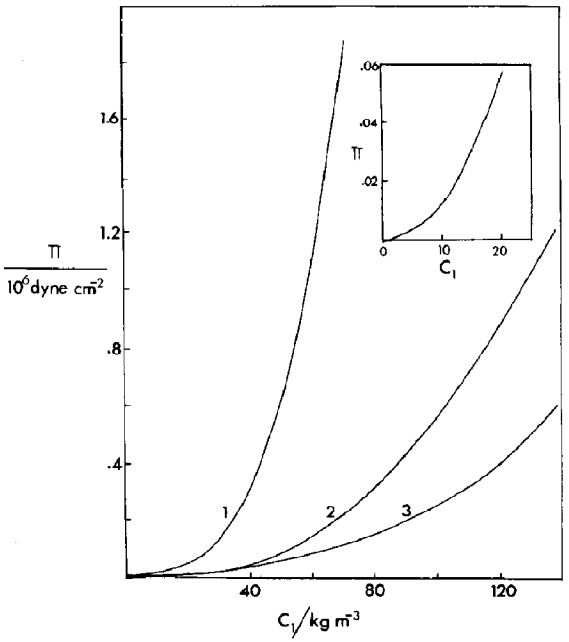

Fig. 4. Osmotic pressure of polyelectrolytes in thermodynamic equilibrium with PGS as a function of polyelectrolyte concentration. (1) PGS from sedimentation-diffusion data [8]. (Inset) PGS from sedimentation equilibrium measurements. (2) Dextran sulfate from sedimentation diffusion data (table 1). (3) Dextran from sedimentation diffusion data [9].

ated when measuring the kinetics of volume flow (fig. 2) where the initial flow obtained 5 min after the start of the experiment was maintained at a steady-state value for over 60 min. There is also quite reasonable agreement between the present results and those from previous experiments, obtained in a different experimental apparatus [5], in the magnitude of the osmotic permeability coefficient at low osmotic pressures for dextrans. The stirred experiments in this newly designed cell show similar patterns of osmotic pressure dependence with a marked decrease in L_p^o with increasing osmotic pressure.

4.2. Variation of L_p^o with osmotic pressure for polyelectrolytes

At present, the direct determination of osmotic pressure at high polymer concentrations is difficult. At this stage, we have resorted to estimates of osmotic pressure through the combination of sedimentation and diffusion experiments (fig. 4). The L_p^o values for dextran sulfate and PGS are shown to decrease with increase in osmotic pressure over the range studied (fig. 5). The values for dextran sulfate are similar to that determined for dextran T70 at the same osmotic pressure (fig. 3) but considerably higher than that obtained with proteoglycan. These relationships show a good qualitative similarity to the variation in the hydrodynamic frictional term $v_1(1-\phi_1)^2 M_1/f_{12}$ of eq. 1 with osmotic pressure (fig. 6) as evaluated from sedimentation velocity analysis. The possible exception is the relatively low values of L_p^o for dextran sulfate which could be rationalised on the basis that the membrane may not be impermeable to this solute as the preparation is extremely heterogeneous with M_n/M_w ratios less than 0.5. The K term in eq. 7 may be calculated from the data in figs 5 and 6 and this is presented in fig. 7. As previously found with uncharged macromolecular solutes [5], the K term is variable but relatively constant for all three macromolecules studied above osmotic pressures of 10^5 dyn cm^{-2}.

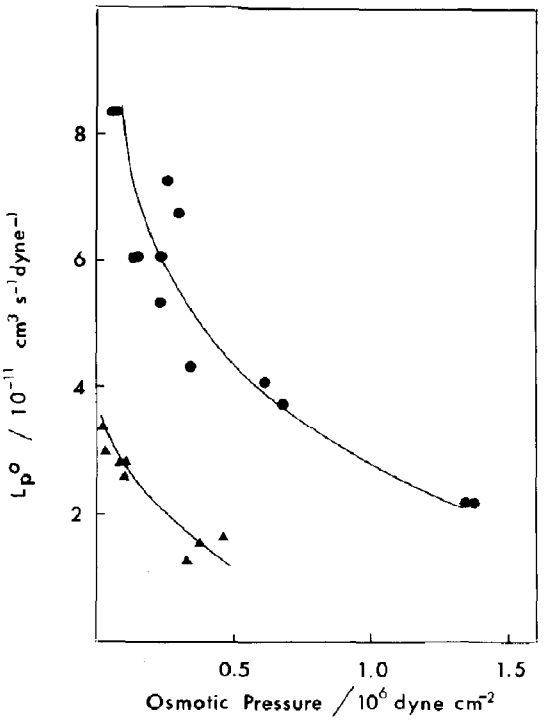

Fig. 5. Variation of the osmotic permeability coefficient, L_p^o, from eq. 3, of a Nuclepore MWCO membrane as a function of osmotic pressure of dextran sulfate T500 (●) and PGS (▲).

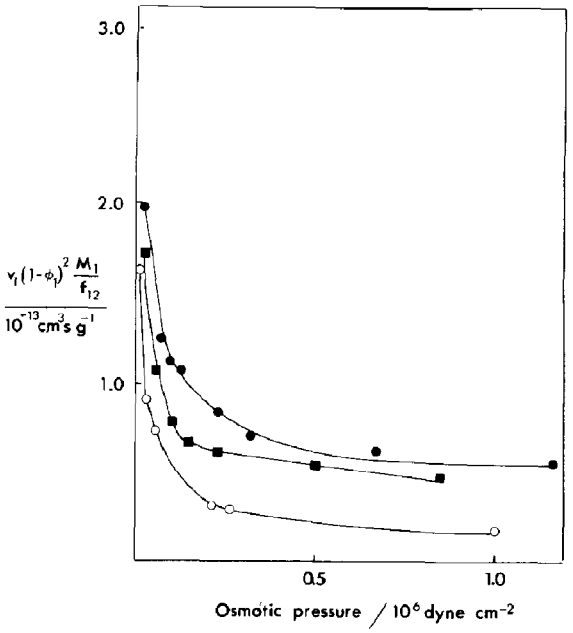

Fig. 6. Variation of $v_1(1-\phi_1)^2 M_1/f_{12}$ of eq. 1 as determined from sedimentation studies (see also ref. 8) as a function of osmotic pressure of the impermeable solutes dextran T500 (■), dextran sulfate T500 (●) and PGS (○).

5. Discussion

It has been previously stated in the literature that a major factor that will influence the magnitude of osmotic flow is the presence of an apparent unstirred layer (or osmotic boundary layer) on the solution side of the membrane [14–16]. This layer represents a thin film of fluid on the solution side of the membrane which is thought to have a lower solute concentration than the bulk solution due to the fact that the osmotic flow of water would advect solute away from the membrane. The layer would give rise to a lower effective osmotic pressure and flow on the basis of solute concentration in the bulk solution. Further, the magnitude of the flow will depend on the efficiency of the stirring motion in the solution to prevent the unstirred layer from forming. Under these circumstances, the ideal flow would yield a concentration-independent L_p^o which has commonly been described in terms of parameters associated with the membrane structure. At present, there is no experimental evidence which demonstrates the nature of the concentration gradients of solute adjacent to the membrane for impermeable membranes (such layers would also be gravitationally unstable with the membrane in the vertical plane as maintained in this study). Further, theoretical models of this osmotic layer are not well defined [16].

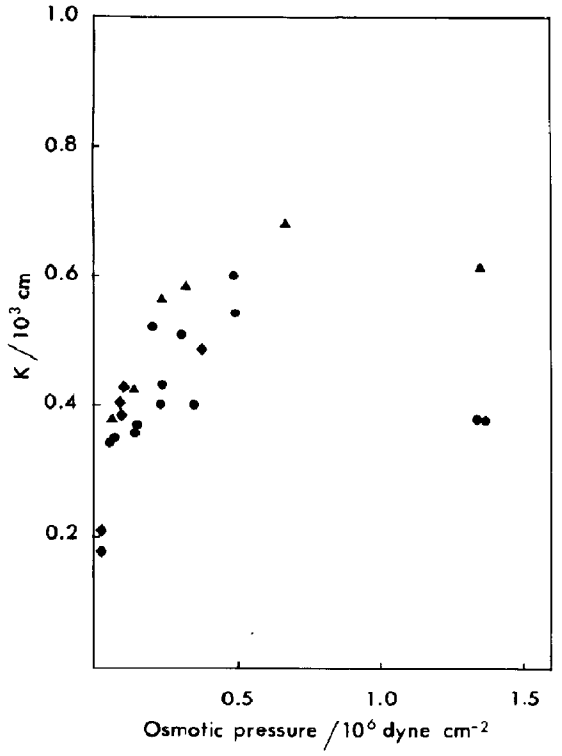

Fig. 7. Variation of the parameter K from eqs 3 and 7 as a function of solute osmotic pressure for dextran sulfate (●), proteoglycan (◆) and dextran (▲).

Our experiments, designed to assess the effect of the apparent unstirred layer, have incorporated an efficient stirring process in the osmotic flow cell and an apparatus which allows for the sensitive monitoring of volume changes associated with osmotic flow. While we have observed an effect of unstirred systems as compared to flow measurements with stirring at 200 rpm, the differences do not account for the magnitude of the marked concentration dependence of L_p^o. We suggest that much of this deviation can be accounted for in an alternative way in terms of describing a thin layer on the solution side of the boundary where solute-solvent exchange occurs which drives flow through the membrane. This layer is distinct from the unstirred layer where it is believed that osmotic flow would push solute away from the membrane. In contrast, the diffusional exchange of solute with solvent generating osmotic flow would initially promote the solute towards the membrane. This represents a clear distinction from the unstirred layer model and with knowledge of the concentration dependence of solute mobility it can consistently account for the variation of L_p^o over a wide range of osmotic pressure. We do note that a similar type of concept, associated with solute-solvent exchange governing osmotic flow in a thin layer on the solution side of the membrane, has been discussed by Soodak and Iverall [4] and earlier by Dainty [17]. Further evidence of solute-solvent exchange being the rate-limiting factor for osmotic flow can be considered in the following argument. An osmotic volume flow of 4×10^{-3} ml min^{-1} (fig. 1) would result in a mean water velocity on the solute side of the membrane of approx. 1.2×10^{-3} cm s^{-1} (u). Since the diffusion coefficient of dextran is about 1×10^{-7} cm^2 s^{-1}

(D), then for a distance l (eq. 5) over which exchange takes place (approx. 40×10^{-7} cm, see following paper) the ratio ul/D would be 0.048. Since stirring effects were small, this line of argument would indicate that the diffusional process, namely, solute-solvent exchange is limiting flow.

The diffusional relaxation of concentration gradients of anionic polyelectrolytes (in thermodynamic equilibrium with phosphate-buffered saline or 0.15 mol dm^{-3} NaCl (used as it mimics physiological conditions)) can be described by equations successfully employed for uncharged polymers by regarding the polyelectrolyte as the electroneutral salt [8,18]. The mutual diffusion has been established as being a function of a thermodynamic term ($\partial \Pi / \partial C_1$) and an hydrodynamic term involving the hydrodynamic frictional coefficient f_{12} (see the appendix). Studies have demonstrated that for neutral polymers the various terms in eqs 1 and 11 exhibit molecular weight independent behaviour in semi-dilute solution; this has also been shown to be the case for polyelectrolytes such as PGS [8] and dextran sulfate (unpublished work). Therefore, the hydrodynamic frictional coefficient of the polyelectrolyte is determined by the mobility of the segments. Further, the contribution of electrolyte dissipation to the mobility of these segments is small [6,7] so that the frictional coefficient of the polyelectrolyte is essentially governed by the same parameters as that for its unchanged counterpart, namely, the chain configuration and effective surface area to volume ratio. On the other hand, factors contributing to the osmotic pressure are essentially those governed by the effective micro-counterions of the polyion as is demonstrated in the comparison of the osmotic pressure of dextran sulfate vs dextran in fig. 4. In addition, the osmotic pressure of PGS is known to be considerably lower at high salt [19].

Studies reported in this investigation establish the hypothesis that the factor governing the dynamic coefficient of osmotic flow is the hydrodynamic frictional coefficient of the polyion as determined by its segmental mobility. This is striking in view of the fact that segment concentration and its contribution to total osmotic pressure will be low considering the major contribution by the micro-counterions. The critical dependence of L_p° on segmental mobility has been substantiated by the observations that for a given osmotic pressure, osmotic flow for proteoglycan is slower than that for dextran and dextran sulfate, which mirrors the same quantitative difference in their hydrodynamic frictional coefficients. In other words, the K values for all these macromolecules are similar, as found in fig. 7.

These studies confirm the previous interpretation of osmotic flow [5] in that it is dependent on the solution properties adjacent to the membrane as embodied in the hydrodynamic frictional coefficient. The use of polyelectrolytes clearly differentiates the roles of the colligative thermodynamic properties of polyelectrolytes as being distinct from the segmental hydrodynamic properties of osmotically active solutes on osmotic flow. The critical role of solute-segmental mobility as being identified with the kinetics of osmotic flow is just another way of regarding solvent mobility on the solution side of the membrane. The fact that polymer segments determine solute diffusion in semi-dilute solutions and in the swelling of gels has already been established in a number of polymer systems [20–22]. We suggest that an analogous situation applies when a polymer (polyelectrolyte) solution is confined by an inert membrane in contact with solvent.

The recognition that the manifestation of osmotic pressure is intimately related to the diffusive mobility of the solute and concentration gradient should have important consequences in considering the dynamics and organisation of osmotically active materials in biological compartments such as membranes and extracellular matrices.

Appendix: The analogy between sedimentation-equilibrium in the ultracentrifuge and water transport across a semipermeable membrane

The basic principles of the hydrodynamics of macromolecular systems should be of value in understanding water transport across membranes in contact with macromolecular solutions. One such experimental technique that was recognized early on as analogous to hydraulic permeabilit

across polymer membranes is that of sedimentation of macromolecules [23,24]. The theoretical treatment of Mijnlieff and Jaspers [25] clearly established the direct relationship between the two types of measurements where the hydraulic permeability k (introduced by D'Arcy [26]) through a porous plug of polymer material or polymer membrane defined as (where solute component is designated 1, solvent water as 2)

$$k = (J_2/\text{grad } P)\eta_2 \tag{A1}$$

where J_2 is the flux of solvent, P the pressure and η_2 the solvent viscosity, is related to the sedimentation coefficient S_1 through the equation

$$k = \frac{\eta_2 S_1}{C_1(1 - v_1/v_2)} \tag{A2}$$

where C_1 denotes the concentration of 1 (mass/volume) and v_i the partial specific volume of i. Surprisingly, there has been a paucity of use of the sedimentation technique in relation to eq. A2 and hydraulic permeability. This appendix extends the analogy of membrane transport to sedimentation equilibrium experiments in the centrifuge. It concludes with the important emphasis of the direct relationship between hydraulic flow and osmotic flow across membranes.

Irreversible thermodynamics provides us with an expression for solute flux (J_1) associated with sedimentation velocity in the centrifuge with respect to a volume (assumed to be the same as that of the cell) fixed frame of reference [27].

$$(J_1) = (S_1)_v C_1 \omega^2 r - (D_1)_v (\partial C_1/\partial r) \tag{A3}$$

where ω is the angular speed of the rotor (rad s^{-1}), r the distance from the center of the rotor and $(D_1)_v$ the mutual diffusion coefficient of solute 1.

At high rotor speeds, the flux J_1 is determined primarily by the sedimentation coefficient, whereas at low rotor speeds equilibrium ($J_1 = 0$) may be easily attained so that a relationship between $(S_1)_v$ and $(D_1)_v$ may be obtained [28]. Irreversible thermodynamic expressions for $(S_1)_v$ derived previously [9], namely

$$(S_1)_v = (1 - \rho v_1)(1 - \phi_1) M_1/f_{12} \tag{A4}$$

$$(D_1)_v = (1 - \phi_1)^2 (M_1/f_{12})(\partial \Pi^*/\partial C_1)_{T,\mu_2} \tag{A5}$$

where

$$\Pi^* = RT\left(C_1/M_1 + A_2^{os} C_1^2 + A_3^{os} C_1^3 + \ldots\right) \tag{A6}$$

may be used to re-express eq. A3 in the form

$$J_1 = (1 - \phi_1) \cdot \left(\frac{M_1}{f_{12}}\right)\left[C_1 \omega^2 (1 - \rho v_1) \frac{(\partial r^2/2)}{\partial r} - (1 - \phi_1)(\partial \Pi^*/\partial r)_{T,\mu_2}\right] \tag{A7}$$

where ϕ_1, M_1 are the volume fraction and molecular weight, respectively, of solute 1, Π^* the osmotic pressure, A_2^{os} and A_3^{os} the standard second and third osmotic virial coefficients, respectively, ρ the solution density, μ_2 the chemical potential of the solvent, and f_{12} the hydrodynamic frictional coefficient of 1 mol of solute with solvent 2 [29].

There are a number of preliminary comments on the important features of eq. A7. The equation does form the basis of using the sedimentation technique to measure osmotic pressure [13]. For a monodisperse polymer preparation, the system behaves like a semipermeable membrane, permeable to solvent only. If there is a degree of polydispersity of the polymer sample the sedimentation equilibrium technique could be considered as analogous to a membrane with partial permeability to solute. We will confine our considerations to the analogy of sedimentation equilibrium to semipermeable membranes only. We also note that when $\omega = 0$ the flux in eq. A7 describes the diffusion process which is expressed as a function of the osmotic pressure gradient and f_{12} the diffusive mobility of the solute. The dual nature of this frictional coefficient is readily evident in that it also describes the viscous dissipation processes occurring in sedimentation (eq. A4). Experimental evaluation of f_{12} indicates that it is quantitatively identical in both mutual and sedimentation [9,30] and that it is markedly concentration dependent, increasing with increasing concentration. Furthermore, the M_1/f_{12} term approaches molecular weight independence at high concentrations, thus demonstrating that water interacting with critical

polymer segments is responsible for the dynamic properties at high macromolecular concentrations. The volume flux (J_v) of water in the sedimentation experiment can also be described by an equation similar to eq. A7 since

$$J_v = J_2 v_2 = -J_1 v_1 \tag{A8}$$

for a volume-fixed frame of reference. We emphasise then that the coefficient describing total volume flow, namely, $(1-\phi_1)M_1/f_{12}$, will determine the rate of flow due to the osmotic pressure gradient (as in diffusion) and the rate of flow due to the pressure gradient created by the centripetal force ($C_1\omega^2(1-\rho v_1)r^2/2$).

The general relation between force X and flow J for a volume-fixed frame of reference is

$$J_2 = L_{22}X_2 = L_{22}\left[\left(\frac{\partial \mu_2}{\partial C_2}\right)_{T,p}\cdot\frac{\partial C_2}{\partial r} + v_2\frac{\partial P}{\partial r}\right] \tag{A9}$$

Using previously reported relationships [9,30], eq. A9 may be expressed as

$$J_2 = \frac{L_{22}v_2}{(1-\phi_1)}\left[(1-\phi_1)\frac{\partial P}{\partial r} - (1-\phi_1)\left(\frac{\partial \Pi^*}{\partial r}\right)_{T,\mu_2}\right] \tag{A10}$$

Comparison of eq. A10 with eq. A7 using eq. A8 requires that

$$L_{22} = -\frac{M_1}{f_{12}}(1-\phi_1)^2\cdot\frac{v_1}{(v_2)^2} \tag{A11}$$

The analogy between the hydraulic permeability component of eq. A10 and sedimentation velocity (with $\partial P/\partial r \gg \partial \Pi^*/\partial r$) has already been discussed earlier whereupon the phenomenological coefficients in both sedimentation and hydraulic permeability are directly related to f_{12}.

We now extend the analogy to the case where a polymer solution is separated from solvent by an inert semipermeable membrane, permeable to solvent. In this case, we recognise that the same processes associated with pressure gradients on the macromolecular solution still exist but that the flow of water will be restricted by the effective membrane geometry. The membrane itself will not influence the relative effectiveness of the hydrostatic pressure or osmotic pressure gradients on the macromolecular solution. We consider the solute-solvent exchange and membrane flow as separate resistances R_s and R_m, respectively, which occur in series. Therefore, with $\Delta P = 0$

$$J_v = L_p^0\Delta\Pi = (1/(R_s+R_m))\Delta\Pi \tag{A12}$$

and where $R_s = l/L_{22}v_2^2$ where l is the distance over which solute-solvent exchange takes place. When the solute-solvent exchange resistance is zero ($C_1 = 0$), then R_m can be measured directly ($R_m = 1/L_p$). We have previously demonstrated [5] that for membranes with R_m values varying by as much as 200-fold, the ratio of L_p^o/L_p ($= R_m/(R_m+R_s)$) is essentially the same for all membranes and approaches unity at low osmotic pressures but falls to values considerably less than unity at high osmotic pressures. These variations can be predicted from the known variation of R_s with osmotic pressure. The similarity of the L_p^o/L_p ratio for the different membranes is not that obvious but is rationalised on the basis that effective membrane area is paramount in governing the magnitude at the solute-solvent exchange process. It is further assumed that differences in membrane thickness were not marked for those membranes.

It is important to emphasise that the manifestation of osmotic pressure across the membrane system relies on the diffusive mobility of the osmotically active solute. In other words, for a given osmotic pressure, a low molecular weight component will generate a faster osmotic flow than a higher molecular weight component [5]. It is clear that these features of hydraulic permeability and osmotic flow have not been described previously. Rather, volume flows have been described by the standard equation [31–33]:

$$J_v = L_p(\Delta P - \Delta\Pi) \tag{A13}$$

where L_p is an hydraulic permeability coefficient which has been assumed to be intrinsically solution and concentration independent and may be related to the geometry of the membrane. The L_p coefficient has been discussed only in terms of the frictional interaction of solvent with the membrane [33]. We suggest that previous interpretations of eq. A13 overlook the contribution made

by the concentration-dependent function associated with solute mobility (and pressure gradients) in the solution outside the membrane.

Acknowledgements

This work was supported by a grant from the Australian Research Grants Scheme, the Monash University Special Research Grant fund and a Commonwealth Postgraduate Scholarship to R.P.W.W. We also acknowledge the expert construction of the osmotic flow cell by the Monash University Medical Dean's Workshop.

References

1 E. Heyer, A. Cass and A. Mauro, Yale J. Biol. Med. 42 (1969) 139.
2 J.S. Schultz, R. Valentine and C.Y. Choi, J. Gen. Physiol. 73 (1979) 49.
3 A. Mauro, Am. J. Physiol. 237 (1979) R110.
4 H. Soodak and A.S. Iberall, Am. J. Physiol. 237 (1979) R114.
5 R.P.W. Williams and W.D. Comper, J. Phys. Chem. 91 (1987) 3443.
6 W.D. Comper and O. Zamparo, Biophys. Chem. 34 (1989) 127.
7 O. Zamparo and W.D. Comper, Arch. Biochem. Biophys. 274 (1989) 259.
8 W.D. Comper and R.P.W. Williams, J. Biol. Chem. 262 (1987) 13464.
9 W.D. Comper, B.N. Preston and P. Daivis, J. Phys. Chem. 90 (1986) 128.
10 J.D. Wells, Proc. R. Soc. Lond. B. 183 (1973) 399.
11 D. Heinegård, Biochim. Biophys. Acta 285 (1972) 181.
12 K.-O. Wik, Thesis, University of Uppsala, Sweden (1979).
13 L.W. Nichol, A.G. Ogston and B.N. Preston, Biochem. J. 102 (1967) 407.
14 T.J. Pedley and J. Fischbarg, J. Theor. Biol. 70 (1978) 427.
15 T.J. Pedley, J. Fluid Mech. 101 (1986) 843.
16 H.A. Massaldi and C.H. Borzi, J. Membrane Sci. 12 (1982) 87.
17 J. Dainty, Symp. Soc. Exp. Biol. 19 (1965) p. 75.
18 K.-O. Wik and W.D. Comper, Biopolymers 21 (1982) 583.
19 J.P.G. Urban, A. Maroudas, M.T. Bayliss and J. Dillon, Biorheology 16 (1979) 447.
20 D.J. Buckley and M. Berger, J. Polym. Sci. 56 (1962) 175.
21 T. Tanaka and D. Fillmore, J. Chem. Phys. 70 (1979) 1214.
22 S. Candau, J. Bastide and M. Delsanti, Adv. Polym. Sci. 44 (1982) 27.
23 R. Signer and H. Egli, Rec. Trav. Chim. 69 (1950) 45.
24 J.H. Fessler and A.G. Ogston, Trans. Faraday Soc. 47 (1951) 667.
25 P.F. Mijnlieff and W.J.M. Jaspers, Trans. Faraday Soc., 67 (1971) 1837.
26 J. D'Arcy, Les fontaines publiques de la ville de Dijon (1856).
27 H. Fujita. Mathematical theory of sedimentation analysis (Academic Press, New York, 1962).
28 T. Svedberg and K.O. Pedersen, The ultracentrifuge (Oxford University Press, London, 1940).
29 K.S. Spiegler, Trans. Faraday Soc. 54 (1958) 1408.
30 W. Brown, P. Stilbs and R.M. Johnsen, J. Polym. Sci. 21 (1983) 1029.
31 O. Kedem and A. Katchalsky, J. Gen. Physiol. 45 (1961) 143.
32 A. Katchalsky and P.F. Curran. Non-equilibrium thermodynamics in biophysics (Harvard University Press, Cambridge, MA, 1967).
33 A. Silberberg. Macromolecules, 13 (1980) 742.